Finite-time localized singularities as a mechanism for turbulent dissipation

Christophe Josserand,[1] Yves Pomeau,[1] and Sergio Rica[1,2,*]
[1]*LadHyX, CNRS & Ecole Polytechnique, UMR 7646, IP Paris, 91128 Palaiseau, France*
[2]*Facultad de Ingeniería y Ciencias and UAI Physics Center, Universidad Adolfo Ibáñez, Avda. Diagonal las Torres 2640, Peñalolén, Santiago, Chile*

(Received 9 October 2019; accepted 28 April 2020; published 28 May 2020)

The nature of the fluctuations of the dissipation rate in fluid turbulence is still under debate. One reason may be that the observed fluctuations are strong events of dissipation, which reveal the trace of spatiotemporal singularities of the Euler equations, which are the zero viscosity limit of ordinary incompressible fluids. Viscosity regularizes these hypothetical singularities, resulting in a chaotic fluctuating state in which the strong events appear randomly in space and time, making the energy dissipation highly fluctuating. Yet, to date, it is not known if smooth initial conditions of the Euler equations with finite energy do or do not blow up in finite time. We overcome this central difficulty by providing a scenario for singularity-mediated turbulence based on the self-focusing nonlinear Schrödinger equation. It avoids the intrinsic difficulty of Euler equations since it is well known that solutions of this NLS equation with smooth initial conditions do blow up in finite time. When adding viscosity, the model shows (i) that dissipation takes place near the singularities only, (ii) that such intense events are random in space and time, (iii) that the mean dissipation rate is almost constant as the viscosity varies, and (iv) the observation of an Obukhov-Kolmogorov spectrum with a power-law dependence together with an intermittent behavior using structure function correlations, in close correspondence with the one measured in fluid turbulence.

DOI: 10.1103/PhysRevFluids.5.054607

I. INTRODUCTION

One of the long-standing problems of classical physics is a thorough understanding of fully developed turbulence. More specifically, with regard to the properties of fluid equations, there is still no explanation for the observed intermittency in flows at high Reynolds number. This phenomenon displays sharp fluctuations in the velocity and acceleration fields [1–3], fluctuations that seem to preclude any theoretical description based on mean-field theory, even a modified one, so that the link between these intermittencies and the turbulent spectrum remains unclear [4].

A possible explanation is that intermittent fluctuations are a consequence of spatiotemporal singularities of the incompressible Euler equations [5]. The addition of dissipation, i.e., viscosity, would regularize these singularities, resulting in a chaotic fluctuating state in space and time, making the energy dissipation rate a highly fluctuating quantity. The problem of the existence of singular solutions of incompressible Euler equations, interesting on its own, dates back at least to the 1920s [6,7]. Several years later, Leray introduced the possibility of the existence of finite-time singularities for the velocity field in the incompressible Navier-Stokes equation, which are pointlike singularities in space-time [8,9]. In contrast with Leray, Onsager later conjectured about the existence of a velocity field as a Weierstrass-like function of space variables [10,11], implying that the velocity

*sergio.rica@uai.cl

is not smooth (i.e., not differentiable) almost everywhere and at almost all times. This assumption is not linked to the fluid equations or even to the existence of finite-time localized singularities. Recently, however, the statistical properties of the velocity field were investigated experimentally and numerically in the context of this Onsager conjecture [12,13].

The existence of finite-time localized singularities in incompressible fluids was a subject of renewed interest in the 1980s because of improvements in computers. Since then, different configurations have been investigated to determine if they exhibit possible singular behaviors, e.g., vortex filaments [14–18] or vortex sheets [19], and Taylor-Green flows [20] (see Ref. [21] for a recent review). In real flows, these singularities, if they exist, could be smoothed by viscosity close to the singularity.

Scenarios of dissipation caused by singularity events have been proposed in different physical contexts: for instance, it is believed that the formation of steep slope deformations on the surface of the sea, leading to "white caps," is responsible for energy dissipation [22,23]. Similarly, ridges, folds, and conical singularities are good candidates for dissipating the energy of strongly vibrating elastic plates [24]. The same is true for the focusing of light in nonlinear media [25] and strong turbulence in plasmas [26–30] and related contexts [31]. Those nonlinear systems share the role of singularities in effective dissipation.

Here we focus on the possible role of Leray-type finite-time singularities in a simpler model of turbulence. One of us (Y.P.) [5,32] has considered such singularities occurring at single points in space and time in a turbulent fluid (assumed to be inviscid), thus having no obvious effect on the time-averaged velocity field. Leray's explicit equations for singularities lead to a very challenging problem that is far from being fully understood. Furthermore, the effect of such singularities on the large-scale dynamics of turbulent flows is still unclear, although it is nicely consistent with the famous Newton v^2-drag law in that it excludes the effect of molecular dissipation in terms of scaling laws [33]. Even though it seems well understood now that these singularities are local sinks of energy, it is still not clear what their role is in the exchange of momentum [3]. In the present paper, we study a model of turbulence in which singularities are present in the inviscid limit in order to shed light on the role of such singularities in the turbulence and the observed intermittency. The motivation, at least for the moment, is therefore to circumvent the difficulty posed by the solutions of the incompressible Euler/Navier-Stokes equations, which makes it difficult to carry out a thorough analytical study of those equations. Over the years, it has been suggested that turbulence should be studied with the help of equations that are simpler than fluid equations. Three famous examples are the Burgers equation [34], the Kuramoto-Sivashinsky (KS) equation [35,36], and the complex Ginzburg-Landau (CGL) [37–39] equation. Each of these equations leads to specific turbulent characterizations. The first one is for a velocity depending on one coordinate and time. Riemann's method of characteristics shows that a smooth initial condition leads to finite-time singularities. Once a small viscosity term is added, this singularity becomes a finite amplitude moving jump [34]. The Burgers equation is thus a fair model for the compressible fluid equations, but not for the incompressible case: there is nothing resembling shock waves in the latter because one does not expect that the three-dimensional (3D) incompressible Navier-Stokes (NS) equations have solutions with stable discontinuities of the velocity gradient. Another model of turbulence in one space dimension is the KS equation, which generates a turbulent state through coupling between the large-scale linear instability and the nonlinearity. However, the dynamics exhibits smooth solutions, and one cannot find a limit where finite-time singularities would play any significant role in its solutions [35,36]. Finally, the complex Ginzburg-Landau equation has been used for modeling turbulence, on the one hand, through the topological defects inherent in this equation, leading to the so-called defect-mediated turbulence [37]. On the other hand, in the same vein as our approach, the CGL equation has been used in the case of the focusing nonlinearity (see the definition below) to mimic some highly fluctuating dynamics [38,39]. However, in these works, only the temporal growths of characteristic quantities were estimated, with no direct links to the statistical properties of the fields, such as a turbulent spectrum and structure functions in particular.

In this paper, we examine the self-focusing nonlinear Schrödinger (NLS) equation, which is a partial differential equation whose behavior resembles what we expect to happen in three-dimensional Euler equations for fluids. However, it is much easier to deal with the numerics and to check various theoretical ideas related to turbulence, particularly those concerning intermittency and dissipation. Our simplified model exhibits well-understood singularities in the inviscid limit, and one can investigate how such singularities are related to the large-scale dynamics. Therefore, universal features in common with fluid turbulence as described by the NS equations may appear and pave the way toward a better understanding of turbulence. In fact, our approach suggests that there is a distinction between the two classes of dynamical systems in that the conserved quantity (mass in NLS, energy in perfect fluids) produced at large scales is dissipated at small scales. In the first class (our NLS model and potentially NS), this quantity is dissipated in the core of singularities by higher-order effects not accounted for at large scales, whereas in the other (typically the KS equation) it cascades smoothly to small scales without finite-time blow-up.

The paper is organized as follows: Section II summarizes the basic model, i.e., we introduce the damped and forced nonlinear Schrödinger equation. In particular, we review the inviscid and unforced limit, which is the usual focusing NLS and the well-understood existence of self-similar finite-time singularities. Section III presents the main results of the turbulent, intermittent behavior of this NLS model, before ending with concluding remarks.

II. THEORETICAL MODEL

We consider the focusing NLS equation with small damping and small forcing:

$$i\frac{\partial\psi}{\partial t} = -\frac{\alpha}{2}\nabla^2\psi - g|\psi|^{2n}\psi - i\nu\Delta^2\psi + f_{k_0}(\boldsymbol{x},t). \tag{1}$$

Here $\psi(\boldsymbol{x},t)$ is a complex field defined in space of dimension D. The parameter $\alpha > 0$ quantifies the dispersion and $g > 0$ quantifies the nonlinear strength. They can be scaled out so that we will use for numerical simulations $\alpha = g = 1$. Without "viscosity" ν and forcing f_{k_0}, one recovers the conservative and reversible NLS equation. Indeed, taking, for instance, a periodic box, it is straightforward to show that the quantities

$$N = \int |\psi|^2 d^D x, \tag{2}$$

$$H = \int \left(\frac{\alpha}{2}|\nabla\psi|^2 - \frac{g}{n+1}|\psi|^{2(n+1)}\right)d^D x, \tag{3}$$

are conserved in time. Notice that while the "mass" N is positive, the sign of the "energy" H is not prescribed for this focusing NLS equation.

The term $-i\nu\Delta^2\psi$ in Eq. (1) denotes damping, which we have chosen to bear two orders of derivation higher than the conservative case ($\nu = 0$), by contrast with the usual CGL equation investigated earlier [38,39]. Finally, $f_{k_0}(\boldsymbol{x},t)$ is a complex force acting at large scales of order $\sim 1/k_0$ (called the integral scale hereafter). Equation (1) is complemented with a smooth initial condition. Figure 1(a) shows a typical x-t diagram of $|\psi(x,t)|^2$ obtained by numerical simulations of Eq. (1): a turbulent regime is observed with large amplitude events localized in space and time. These events display strong gradients with very strong local dissipation [defined below (12)], as displayed in Fig. 1(b). We solve the nonlinear Schrödinger equation (1) with a standard pseudospectral scheme, where the nonlinear term is solved in real space, while the linear terms (Laplacian and bi-Laplacian) are solved in Fourier space. All simulations presented in the paper are for $n = 3$ in a one-dimensional domain of size L with periodic boundary conditions. The forcing f_{k_0} is a white noise in time of amplitude a and a variance $a^2/6$ acting only for wave numbers $|k| \leqslant k_0$. Typically the runs correspond for 2048 allocation points and a system size of $L = 307.2$, $k_0 = 0.3$, $a = 0.01$, and $dx = 0.15$. Finally, the viscosities vary from $\nu = 2.5 \times 10^{-3}$ up to $\nu = 2.5 \times 10^{-6}$. We have checked that higher resolutions in space and time do not change quantitatively the results.

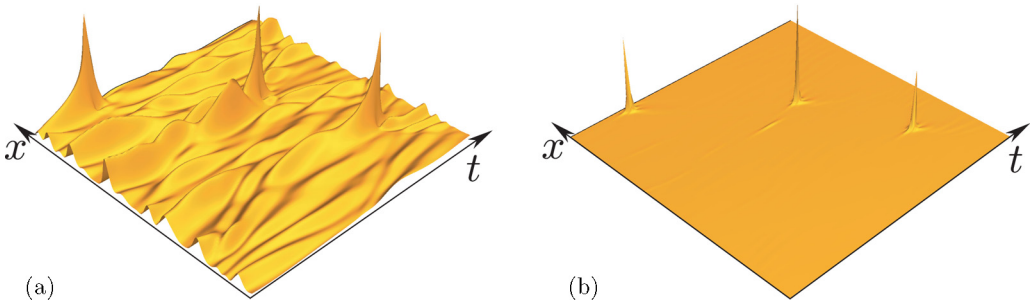

FIG. 1. x-t diagram for numerical simulations of (1) for $D = 1$ and $n = 3$. (a) $|\psi(x,t)|^2$ and (b) the local and instantaneous dissipation $\epsilon(x,t)$. The dissipation is strong near the large density events displayed in (a) and negligible otherwise. As a scale reference, the maximum value of $\max\{|\psi(x,t)|^2\} \approx 6.67$, while for the dissipation $\max\{\epsilon(x,t)\} \approx 600$. The simulations use a pseudospectral method with 1024 modes, a mesh size $dx = 0.05$ (the periodic domain is of size $L = 51.2$), $dt = 10^{-6}$, $\nu = 2.5 \times 10^{-5}$, and $g = \alpha = 1$, using a time-splitting scheme: the nonlinear term is solved in real space, while the derivative is solved in the Fourier space. Finally, the random forcing acts for wave numbers $k < k_0 = 0.3$ with a forcing amplitude $a = 0.01$, and is added in the Fourier space integration step.

A. The inviscid case: Wave collapse

One exciting feature of the model (1) is that in this conservative limit ($f_{k_0} = 0$ and $\nu = 0$), the solutions of (1) may display a finite-time singularity at a point (a position and a time that are hard to predict). More precisely, if $2 \leqslant nD < 2(n+1)$ and for smooth initial conditions such that initially $H < 0$, then the solution of (1) blows up at a point (the solution and its gradient become infinite) in finite time, the case $nD = 2$ representing a critical collapse. Moreover, the singularity formation is self-similar so that its amplitude increases while the size of the blow-up region decreases [40,41]. In our model, Eq. (1), this singularity is avoided thanks to the viscous term, and a turbulent regime appears where forcing and dissipation balance each other. Although the structure of this singular dynamics was studied earlier, we recall in this section the main arguments and results for the sake of consistency (for more details, see [40–44]).

The argument for a finite-time singularity follows from Refs. [43,44]: let us define $\langle|\boldsymbol{x}|^2\rangle = \int |\boldsymbol{x}|^2 |\psi(\boldsymbol{x},t)|^2 d^D\boldsymbol{x}$. Then we obtain (here $\alpha = g = 1$)

$$\frac{d^2}{dt^2}\langle|\boldsymbol{x}|^2\rangle = 8\left(H - \frac{nD-2}{2(n+1)}\int |\psi(\boldsymbol{x},t)|^{2(n+1)} d^D\boldsymbol{x}\right),$$

therefore if $nD > 2$ one has $\frac{d^2\langle|\boldsymbol{x}|^2\rangle}{dt^2} \leqslant 8H$. Moreover, because H is constant, $\langle|\boldsymbol{x}|^2\rangle \leqslant 4Ht^2 + c_1 t + c_0$, thus, if initially $H \leqslant 0$, then a critical time t_c exists such that $\langle|\boldsymbol{x}|^2\rangle \to 0$ as $t \to t_c$. Because of the Cauchy-Schwartz inequality applied to $\int |\psi|^2 dx = (1/D)\int (\boldsymbol{\nabla}\cdot x)|\psi|^2) dx = -(1/d)\int x \cdot \boldsymbol{\nabla}|\psi|^2 dx$, this result implies that $\int |\boldsymbol{\nabla}\psi|^2 d^D x \to \infty$ as $t \to t_c$, indicating a finite-time singularity. Moreover, it can be argued that the Hamiltonian of the singularity solution must vanish at the collapse in order to ensure conservation of energy for this solution.

There is clear evidence of the existence of self-similar finite-time blow-up solutions with an amplitude that increases in a contracting region that is uniformly narrow just before the collapse time [40,41]. Indeed, following [40,41], we can seek a self-similar radially symmetric solution ($r = |\boldsymbol{x}|$) in the form

$$\psi(r,t) = \frac{1}{(t_c - t)^{1/2n}}\Phi\left(\frac{r}{(t_c-t)^{1/2}}, -\ln(t_c - t)\right). \tag{4}$$

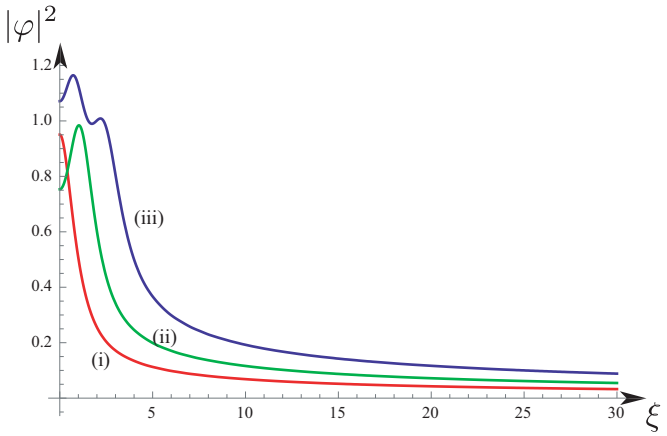

FIG. 2. Numerical calculation of the ordinary differential equation (5) with the boundary conditions (6) for the parameters (i) $\varphi_0 = 0.975$ and $\lambda = 0.3598$; (ii) $\varphi_0 = 0.8675$ and $\lambda = 0.707$; and (iii) $\varphi_0 = 1.035$ and $\lambda = 1.4175$. The calculated solutions represent an example of nonoscillatory solutions of (5) with the boundary conditions (6), however only (i) satisfies the energy condition $\mathcal{H}_0 = 0$ discussed below.

The function $\Phi(\xi, \tau)$ depends then only on the stretched variable $\xi = r/(t_c - t)^{1/2}$ and the log-time $\tau = -\ln(t_c - t)$, and it is a solution of the partial differential equation:

$$i\frac{\partial}{\partial\tau}\Phi(\xi,\tau) + \frac{i}{2}\left(\frac{1}{n} + \xi\frac{\partial}{\partial\xi}\right)\Phi = -\frac{1}{2}\left(\frac{\partial^2\Phi}{\partial\xi^2} + \frac{D-1}{\xi}\frac{\partial\Phi}{\partial\xi}\right) - |\Phi|^{2n}\Phi.$$

This equation admits "oscillatory" solutions in τ of the form $\Phi(\xi, \tau) = e^{i\lambda\tau}\varphi(\xi)$, where $\varphi(\xi)$ satisfies the ordinary differential equation

$$-\lambda\varphi + \frac{i}{2}\left(\frac{1}{n}\varphi + \xi\varphi'\right) = -\frac{1}{2}\left(\varphi'' + \frac{D-1}{\xi}\varphi'\right) - |\varphi|^{2n}\varphi, \tag{5}$$

which is complemented by the boundary conditions

$$\varphi(0) = \varphi_0, \;\; \varphi'(0) = 0, \;\; \text{and } \varphi(\xi) \sim \xi^{-1/n}, \;\; \xi \to \infty. \tag{6}$$

Because of the phase invariance of (5), one can set φ_0 real, and integrating Eq. (5) for any given pair of (λ, φ_0) generates in general oscillatory functions (in ξ) in the limit $\xi \to \infty$. The selection mechanism of the solutions follows by simply eliminating the functions that are oscillating in this asymptotic limit $\xi \to \infty$, leading to a family of solutions associated with each pair of (λ, φ_0).

Generally speaking for this class of problems, the set of pairs (λ, φ_0) satisfying both Eq. (5) and the boundary conditions (6) is infinite but countable, and Fig. 2 shows three of these solutions.

Near the wave collapse, the conserved quantities become $N = (t_c - t)^{D/2-1/n}\mathcal{N}_0$. Because $nD > 2$, $N \to 0$ as $t \to t_c$, implying that the mass or wave action converges to zero at the singularity. On the other hand, H scales as $H = (t_c - t)^{D/2-1/n-1}\mathcal{H}_0$, hence it may diverge for $2 < nD < 2(n+1)$, and in this case it is necessary to impose the supplementary condition

$$\mathcal{H}_0 = \int_0^\infty \left(\frac{1}{2}|\varphi'|^2 - \frac{1}{n+1}|\varphi|^{2(n+1)}\right)\xi^{D-1}d\xi \equiv 0. \tag{7}$$

Therefore, the solution selected by the dynamics must not only satisfy Eq. (5) with the boundary condition (6), but also the important restriction (7), which limits strongly the number of acceptable solutions. For instance, for the numerical solutions shown in Fig. 2, only the first case (i) satisfies this condition (7).

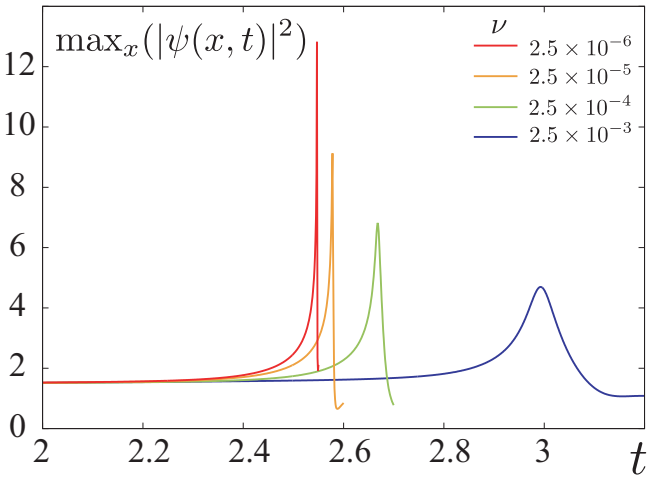

FIG. 3. Time evolution of $|\psi_0(t)|^2 = \max_x(|\psi(x,t)|^2)$, solution of (1) with zero forcing and starting at $t = 0$ with a smooth initial condition $\psi(x,0) = 1 + 0.1\cos(\frac{2\pi x}{L})$, where $L = 51.2$ is the size of the periodic box, $g = \alpha = 1$, for various ν. The dynamics shows a peak reminiscent of the self-similar singular dynamics of the inviscid case (the peak is located earlier and its amplitude is larger as ν decreases). The mesh size has been adapted in order to solve the high-density peaks, and the case $\nu = 2.5 \times 10^{-4}$ has been slightly shifted in time for clarity.

B. Basic linear instability mechanism

The formation of the finite-time singularity discussed in the previous section is preceded by a long-wave instability mechanism that in the end cannot be saturated by the nonlinearities, so that the dynamics end because of the singular behavior. Indeed, in the absence of forcing, $f_{k_0} = 0$, the model (1) admits uniform solutions $\sqrt{\varrho_0}e^{ig\varrho_0^n t}$, where $\sqrt{\varrho_0}$ is constant. The linear stability analysis of periodic perturbations leads to the following dispersion relation:

$$\sigma_k^{(\pm)} = -\nu k^4 \pm \sqrt{\alpha n g \varrho_0^n k^2 - \alpha^2 k^4/4}. \tag{8}$$

In the long wave limit, the eigenvalue

$$\sigma_k^{(+)} \approx -\nu k^4 + |k|\sqrt{g\alpha n \varrho_0^n}$$

develops a long wave modulation instability for all $\nu > 0$. Therefore, the uniform solution is linearly unstable for any smooth initial condition, and it can trigger the self-focusing mechanism for wave collapse as described above. As the solution becomes narrow and broad in amplitude, the viscous dissipation becomes more efficient and, eventually, avoids the inviscid blow-up. This instability mechanism can be seen in numerical simulations by following the time evolution of the equation, starting from a smooth bump initial condition. Although the model exhibits singularities for any space dimension, we will focus next on the 1D version since it displays the essence of the dynamics and allows for high accuracy numerical simulations (we take the supercritical regime $D = 1$ and $n = 3$ for all the numerical results shown below). Figure 3 plots the maxima: $|\psi_0(t)|^2 = \max_x(|\psi(x,t)|^2)$ as functions of time for different viscosities ν: we observe that the smaller the viscosity, the sooner and the higher is the peak of $|\psi_0(t)|^2$. This indicates that the viscosity indeed cures the singularity of the inviscid equation in such a way that the peak intensity diverges as the viscosity vanishes.

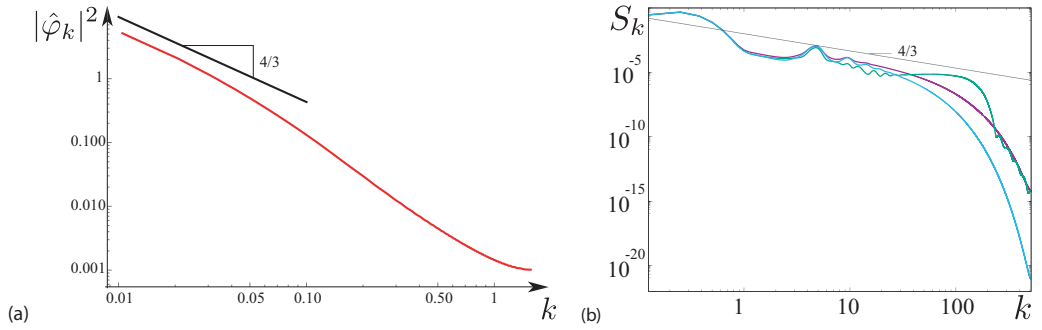

FIG. 4. (a) Numerical calculation of the wave spectrum of the self-similar solution of Fig. 2 for the solution (i) of the ordinary differential equation (5) already plotted in Fig. 2. Note the $k^{-4/3}$ spectrum for the long-wave behavior. (b) Plots of the instantaneous 1D average spectrum S_k as a function of k for times near the peak for the smallest viscosity $\nu = 2.5 \times 10^{-6}$ shown in Fig. 3. From bottom to top, the blue curve is the available time-step just before, $t = 2.546$, the purple one is on the peak, $t = 2.547$, and the green is for the time-step just after the peak, $t = 2.548$. The straight line indicates the slope $k^{-4/3}$ that can be deduced from the self-similar structure of the singularity.

C. Wave collapse spectrum

We define the instantaneous Fourier spectrum $S_k(t)$ by

$$S_k(t) \equiv \langle |\hat{\psi}_{\boldsymbol{k}}|^2 \rangle, \tag{9}$$

where the Fourier transform reads

$$\hat{\psi}_{\boldsymbol{k}}(t) = \frac{1}{L^{D/2}} \int \psi(\boldsymbol{x}, t) e^{-i\boldsymbol{k}\cdot\boldsymbol{x}} d\boldsymbol{x},$$

and the brackets $\langle \cdots \rangle$ stand for a mean angular average [45]. The Fourier transform of the self-similar solution (4) reads

$$\hat{\psi}_k(t) \sim (t_c - t)^{D/2 - 1/2n - i\lambda} \hat{\varphi}(k(t_c - t)^{1/2}). \tag{10}$$

In the limit $t \to t_c$, $|\hat{\varphi}(u)| \sim u^{-(D-1/n)}$ so that the full spectrum is time-independent: $|\hat{\psi}_k|^2 \sim k^{-2(D-1/n)}$, leading to the observed spectrum $|\hat{\psi}_k|^2 \sim k^{-4/3}$ (for $D = 1$ and $n = 3$) in Fig. 4(a).

This dynamical spectrum is observed in numerical simulations of Fig. 3. Indeed, as shown in Fig. 4(b), we observe that the spectrum just before the peak and the one on the peak present a smooth behavior compatible with the scaling law $k^{-4/3}$ that can be deduced from the self-similar regime. However, the spectrum for the time step just after the peak exhibits a different behavior with the rapid formation of small-scale (large k) fluctuations, as demonstrated by the oscillations observed after the peaks in Fig. 1.

III. TURBULENT BEHAVIOR

Given the dynamics of the NLS equation, it is tempting to investigate the existence of a turbulent regime that would arise as a balance between the singular dynamics and the dissipation. By "turbulence," we mean a disordered or chaotic spatiotemporal behavior given by the solutions of partial differential equations [like (1)] starting from a smooth initial condition. In this turbulent regime, mass (N) and energy (H) are injected at large scale by a forcing term $f_{k_0}(x, t)$, while the viscous term dissipates at small scales.

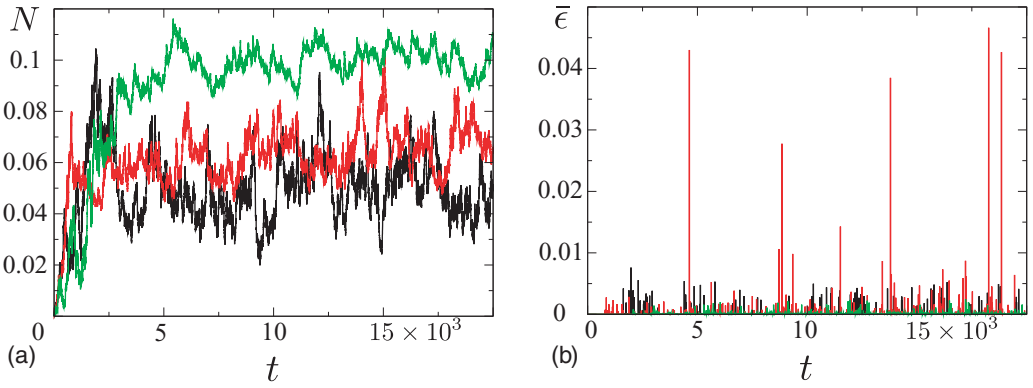

FIG. 5. (a) Time evolution of the mean density $\bar{N}(t)$ for three different values of $\nu = 10^{-5}$ (black curve), $\nu = 2.5 \times 10^{-4}$ (green curve), and $\nu = 2.5 \times 10^{-2}$ (red curve); (b) the mean mass dissipation $\bar{\epsilon}(t)$ is also computed and plotted as a function of time for the same values of the viscosity (same curve color). The numerics is for the same parameters as Fig. 1 but for $L = 307.2$, $dx = 0.15$. We have checked that higher resolutions in space and time do not change qualitatively the results.

A. Dissipation rate

Since the energy may be positive or negative, the interesting quantity to investigate in this turbulent process is the mass N (2), which is positively defined. Following the NLS equation (1), the time variation of N reads

$$\frac{dN}{dt} = -\int \epsilon(\boldsymbol{x}, t)\, d^D\boldsymbol{x} + i \int \left(\psi f_{k_0}^* - \psi^* f_{k_0}\right) d^D\boldsymbol{x}, \tag{11}$$

with

$$\epsilon(\boldsymbol{x}, t) = 2\nu |\Delta\psi|^2. \tag{12}$$

Therefore, in strong analogy with fluids, the dissipation density $-\epsilon(\boldsymbol{x}, t)$ is strictly negative while the forcing can be positive or negative. On the contrary, time derivatives of Eq. (3) can also be developed, but it does not display a simple form such as (11). Thus, in what follows we will focus on $N(t)$ and its dissipation balance (11) and (12).

Numerical simulations in 1D show the existence of a permanent turbulent regime as illustrated in Fig. 5. More precisely, it shows the (space)-averaged density and dissipation

$$\bar{N}(t) = \frac{1}{L}\int_0^L |\psi|^2 dx, \tag{13}$$

$$\bar{\epsilon}(t) = 2\nu \frac{1}{L}\int_0^L |\partial_{xx}\psi|^2 dx \tag{14}$$

as a function of time for three different values of the viscosity ν. Throughout the paper, we denote the spatial average of a quantity q by $\bar{q}$, and the temporal averages by $\langle q \rangle$, so that $\langle \bar{\epsilon} \rangle$ denotes the spatiotemporal average. Figure 5(a) shows that a stationary statistical regime is rapidly reached where $\bar{N}(t)$ fluctuates around a mean value that is not strongly dependent on the viscosity. The mean (in space) dissipation, Fig. 5(b), exhibits a (statistically steady) randomly distributed sequence of peaks, in close correspondence with turbulent dissipation [2]. These peaks correspond to the formation of singularities stopped by the viscosity. Indeed, it is possible to estimate the dissipation rate for the singular solution (4), yielding

$$\bar{\epsilon}(t) = 2\nu (t_c - t)^{D/2-1/n-2} \int_0^\infty |\Delta_\xi \varphi|^2 \xi^{D-1} d\xi.$$

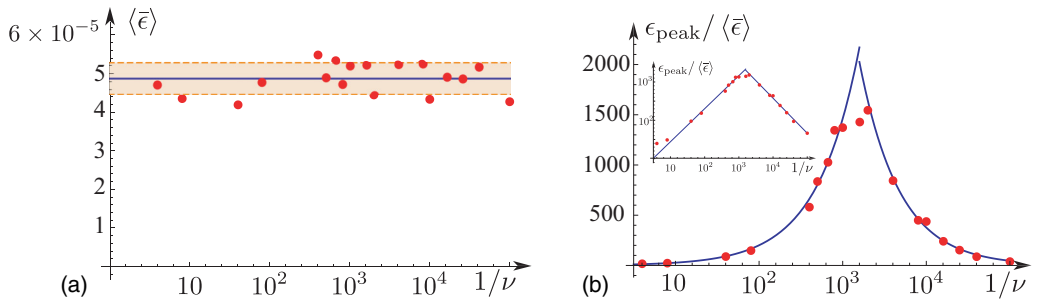

FIG. 6. (a) Mean dissipation rate $\langle \bar{\epsilon} \rangle$ as a function of viscosity. One notices that the mean dissipation rate is $\langle \bar{\epsilon} \rangle = (4.87 \pm 0.40) \times 10^{-5}$ and almost independent of viscosity. (b) Mean peak dissipation created by the intermittent events, normalized by the mean dissipation rate, as a function of viscosity. One observes that the peak events may be as large as 2000 times the mean dissipation rate. The inset suggests a power law $\epsilon_{\text{peak}}/\langle \bar{\epsilon} \rangle \sim A_{\pm}|\nu_c/\nu|^{\eta_{\pm}}$, with $\eta_+ \approx -0.91$ for $\nu_c/\nu > 1$, $\eta_- \approx 0.86$ for $\nu_c/\nu < 1$, and $\nu_c \approx 6.56 \times 10^{-4}$.

That is, $\bar{\epsilon}(t) \sim (t_c - t)^{-11/6}$ for $D = 1$ and $n = 3$ as studied here, consistent with the sharp peak of dissipation observed in the numerics. The total dissipation rate would diverge in time as $t \to t_c$, the viscosity regularizing this singular behavior. Remarkably, in our numerics we observe that the dissipation peak decreases with the viscosity, while the peak frequency increases so that the spatiotemporal averaged dissipation remains finite as $\nu \to 0$.

As ν varies, keeping all the other parameters constant, we observe that the overall picture is preserved. In particular, the mean dissipation rate, $\langle \bar{\epsilon} \rangle$ (averaged in time and space), varies only slightly with the viscosity, as shown in Fig. 6(a). This indicates that the injection determines this quantity while the dissipation process adapts automatically as ν varies. It corresponds to the ideal situation expected in fully developed turbulence of anomalous dissipation, where it converges to a constant value as the viscosity decreases [46]. On the other hand, the amplitude of the dissipation peaks exhibits a nonmonotonic dependence with the viscosity, as shown in Fig. 6(b), where the average of the dissipation peaks normalized by the mean dissipation rate $\langle \bar{\epsilon} \rangle$ is plotted as a function of $1/\nu$. As $\nu \to 0$, the dissipation peaks decrease, as displayed in Fig. 5(b).

B. Kolmogorov-Obukhov spectrum

In the current scenario, Eq. (1) displays a turbulent behavior in the sense that the injected mass at large scales is eventually dissipated at the small ones. However, as seen above, the dissipation mechanism does not *a priori* appear as a cascade regime with a constant mass flux since it depends on random peaks reminiscent of the singular behavior of the inviscid model. It is interesting to measure the spectrum (9) that will be obtained for this intermittent spatiotemporal turbulence. The spectrum S_k evolution is ruled by the general transport equation (in Fourier space):

$$\frac{\partial S_k}{\partial t} = -\frac{\partial Q_k}{\partial k} - 2\nu k^4 S_k + F_k, \tag{15}$$

which relates the flux Q_k, the dissipation $-2\nu k^4 S_k$, and the injection $F_k = \text{Im}[2i\psi_{\boldsymbol{k}} \bar{f}_{-\boldsymbol{k}}]$. Dissipation acts mostly on the small scales (large k such that $\nu k^4 \gg \alpha k^2$) while injection acts only on the large scales ($|k| < k_0$) defining an inertial window where dissipation and injection are negligible. Similarly to what has been observed for the spectrum variation near a peak [see Fig. 4(b)] and because of the existence of intermittent collapses, the instantaneous spectrum $S_k(t)$ fluctuates significantly with time at short scales, while the large-scale part of the spectrum is roughly independent of time. It is thus more relevant to investigate the temporal averaged spectrum $\langle S_k \rangle$ in the statistically steady regime, which will play the role of the Kolmogorov spectrum in fluid

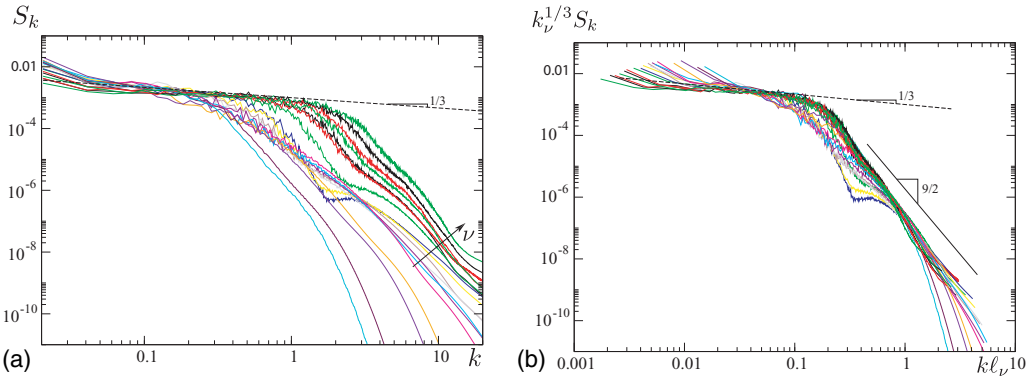

FIG. 7. (a) Time-averaged spectra $\langle S_k \rangle$ for 18 different values of the viscosities, ranging from $\nu = 2.5 \times 10^{-6}$ up to $\nu = 0.25$. The spectra seem to follow the same scaling law $\langle S_k \rangle \sim k^{-1/3}$ over a range that goes from the injection scale toward a scale that depends on ν. (b) The rescaled spectra $\ell_\nu^{-1/3} \langle S_k \rangle$ as a function of the rescaled wave number $k\ell_\nu$, where $\ell_\nu \sim (\nu/\bar{\epsilon})^{3/14}$ is the Kolmogorov dissipation scale. The dashed line indicates the $k^{-1/3}$ and $k^{-9/2}$ behavior, respectively.

turbulence. Thus $\langle S_k \rangle$ is time-independent and the averaged flux $\langle Q_k \rangle$ becomes constant in the inertial window in k. Finally, the behaviors at large and small k impose $\langle Q_k \rangle = -2\nu \int_k^\infty k^4 \langle S_k \rangle dk \equiv -\langle \bar{\epsilon} \rangle$. This statistically constant mass flux suggests that a cascade process is at play in the averaged dynamics, while the high fluctuations of the instantaneous spectrum $S_k(t)$ witness the intermittent structure of this cascade.

Figure 7(a) displays such Kolmogorov spectra obtained from numerical simulations of (1) with varying ν, the other parameters being the same as in Figs. 5 and 6. We observe that these spectra are almost similar for small k while their extension in k increases as the viscosity decreases. It draws an asymptotic master curve that exhibits a scaling consistent with $\langle S_k \rangle \sim k^{-1/3}$ at a small k corresponding to the inertial range. As ν decreases, the size of this inertial range expands. Remarkably, when the amplitude of the forcing a is varied at fixed viscosity, changing $\langle \bar{\epsilon} \rangle$, we observe the same independence of the spectra with $\langle \bar{\epsilon} \rangle$.

A Kolmogorov-like argument is not sufficient to predict such a spectrum because Eq. (1) has two distinct conservation laws, leading to another dimensionless number. By dimensional analysis and according to the numerical observation that the final spectrum does not depend on $\langle \bar{\epsilon} \rangle$, one concludes that the spectrum

$$\langle S_k \rangle \sim (\alpha/g^4)^{1/3} k^{-1/3}.$$

It is worthwhile to emphasize that this final argument is different from that for wave turbulence so that our spectrum is not at all of this type [47]. More importantly, classical arguments of wave turbulence would suggest an inverse cascade of mass for the NLS equation, while the singular collapse presented here induces an effective cascade of mass toward small scales. This $k^{-1/3}$ scaling is eventually different from that of the singularity observed in Fig. 4, suggesting a subtle average of the singularity spectrum that might be similar to the one proposed in vortex bursting [48,49].

This scaling is well defined in the inertial range k until a critical scale ℓ_ν, at which the local dissipation rate balances the mean one: $\langle \bar{\epsilon} \rangle \sim \nu |\Delta \psi|^2$, leading to

$$\ell_\nu \sim \left[\left(\frac{g}{\alpha} \right)^{1/3} \frac{\bar{\epsilon}}{\nu} \right]^{-\frac{3}{14}}.$$

This provides an estimate of the scale extent of the spectrum for our 1D problem suggesting the general shape

$$\langle S_k \rangle = \left(\frac{\alpha}{g^4}\right)^{1/3} \ell_\nu^{1/3} G(k\ell_\nu). \tag{16}$$

The master scaling relation (16) is tested in the inset of Fig. 7 where all rescaled spectra $\ell_\nu^{-1/3}\langle S_k\rangle$ are plotted as a function of the rescaled wave number $k\ell_\nu$ for different values of the viscosities. Numerically, we observe a reasonable collapse of the spectra for the smallest values of the viscosities, where $G(\eta) \sim \eta^{-1/3}$ in the inertial range, showing the self-similar structure of the turbulence. In addition, the small-scale spectra (large k) follow a power-law behavior $G(\eta) \sim \eta^{-9/2}$. Therefore, the shape of this turbulent spectrum is consistent with a Kolmogorov-type cascade spectrum and does not put in evidence the genuine singular dynamics of Eq. (1).

C. Structure functions and intermittency

Intermittency of the dynamics can usually be characterized using high-order structure functions $g_p(r)$, defined here thanks to the second-order difference $\delta^2\psi(x,r) = \psi(x+r) + \psi(x-r) - 2\psi(x)$, following [50,51]

$$g_p(r) = \overline{|\delta^2\psi(x,r)|^p} = \overline{|\psi(x+r) + \psi(x-r) - 2\psi(x)|^p}. \tag{17}$$

As defined, the structure functions are particularly sensitive to the high amplitude field at large p. Eventually, the narrow peaks of the dynamics should dictate the properties of the structure functions at high p. From the spectrum we can infer that the second-order structure function $g_2(r) \sim r^{7/2}$ for small r (where dissipation dominates) since

$$\begin{aligned} g_2(r) &= \frac{1}{L}\int_0^L dx |\psi(x+r) + \psi(x-r) - 2\psi(x)|^2 \\ &= \frac{4}{L^2}\int dx \sum_{k,k'} e^{i(k-k')x}\hat{\psi}_k\hat{\psi}^*_{k'}[\cos(kr)-1][\cos(k'r)-1], \\ &= \frac{4}{L}\sum_k |\hat{\psi}_k|^2[1-\cos(kr)]^2 \sim r^{7/2}\int (kr)^{-9/2} d(kr) \sim r^{7/2}, \end{aligned}$$

where we have used the inverse Fourier transform relation $\psi(x,t) = \frac{1}{\sqrt{L}}\sum_k \hat{\psi}_k e^{ikx}$, where the sum is for $k = \frac{2\pi i}{L}$, with $i \in \mathcal{Z}$. The $r^{7/2}$ is deduced using the behavior at large k of $\langle S_k\rangle \sim k^{-9/2}$ for $|\hat{\psi}_k|^2$ and by taking the integral limit of the sum in k for simplicity. Figure 8 shows the structure functions for $p = 2$, 6, 8 and 10 for a small value of the viscosity $\nu = 10^{-5}$. The scaling behavior for $g_2(r)$ is observed at small scales, while the structure function saturates at large r, reminiscent of the random fluctuations of the wave function. Indeed, at large r, the wave functions separated by the distance r are totally uncorrelated so that $\overline{|\delta^2\psi(x,r)|^2}$ converges to a constant value related to the mean density of the solution $\overline{|\delta^2\psi(x,r)|^2} \sim 6\overline{|\psi(x)|^2}$. More interestingly, the short-scale behavior of the structure functions varies abruptly for large p showing a peak that grows as p increases (see the inset of Fig. 8). We interpret this peak as the signature of the existence of quasisingularity events in space and time which create large and narrow density peaks. Indeed, in principle, the measure of large-order structure functions may be useful to identify singularities in high Reynolds number fluid motion [32].

D. The pertinence of this scenario with turbulence in real fluids

Along the same lines as the original ideas of Kolmogorov on turbulence in fluids [52], our model displays a set of hierarchical "pulsations" or fluctuations and instabilities at a given length scale, ℓ,

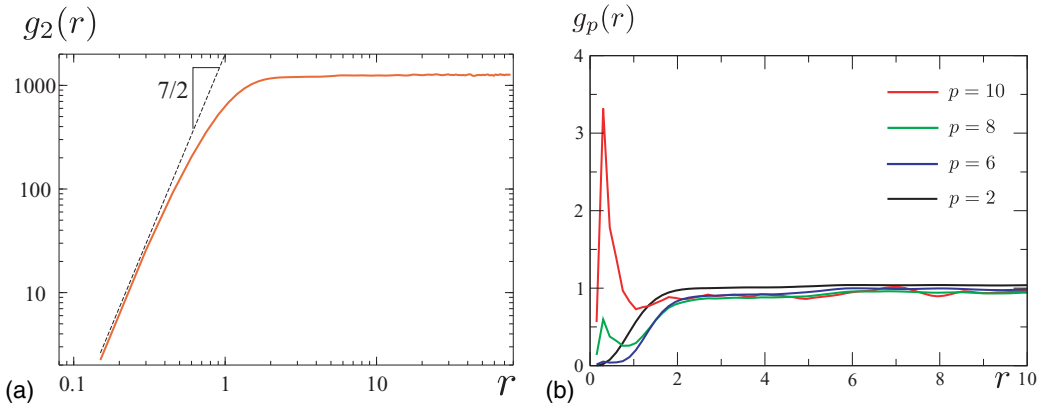

FIG. 8. Structure function $g_p(r)$ as function of r for $\nu = 10^{-5}$. Part (a) shows, in a log-log plot, the function $g_2(r)$ where the short-scale behavior $g_2(r) \propto r^{7/2}$ is reminiscent of the viscous behavior of the spectrum $S_k \propto k^{-9/2}$. Part (b) shows the higher-order structure functions $g_p(r)$ in a linear plot for $p = 2,\ 6,\ 8$, and 10, normalized by their asymptotic values reached for large r. A peak emerges at small r for $p = 8$ and more clearly for $p = 10$.

that dominate the statistical behavior of the turbulent fluid motion. Equation (8) suggests a possible picture for the growth of instabilities and quasisingularities in conditions of a random distribution of the field $|\psi|^2$. Indeed, the scaling law for the local growth of the instability must be such that the wave number $k < \sqrt{n\alpha g|\psi|^{2n}}$. Therefore, whenever $|\psi|^2$ fluctuates in space, the instability can grow if its wavelength satisfies $\ell > 1/\sqrt{n\alpha g\langle|\psi|^{2n}\rangle_\ell}$, where $\langle|\psi|^{2n}\rangle_\ell$ stands for the average value of $|\psi|^{2n}$ over a volume (of linear size ℓ) where the instability grows. This instability reaches rapidly a strongly nonlinear regime that would yield a finite-time singularity without the viscosity term. With viscosity this growth is stopped, and mass, $\langle|\psi|^2\rangle_\ell$, is locally lost on a short time scale $\sim\ell^4/\nu$. As a consequence of this loss of mass in the unstable domain, $\langle|\psi|^{2n}\rangle_\ell$ will decrease to a smaller value bringing ψ back to the stable domain. Afterward, following the dynamics of (1), $|\psi|^2$ will start again to grow either by neighboring diffusion (as is likely to occur in real turbulence) and/or by external forcing.

This mechanism may be amplified in the large-n limit, whereas in Eq. (1) the nonlinear term may be neglected for $|\psi| < 1$, but the nonlinear focusing mechanism becomes stronger whereas $|\psi| > 1$ (even for the smallest possible wavelength). The physics behind this limit resembles an activation process: if the forcing is large enough such that $|\psi| > 1$, the local value of $|\psi|$ increases dramatically, but diffusion acts to decrease the local value of $|\psi|$, reestablishing a permanent dynamics of diffusion-regularized singularities, an idea that we plan to explore in the future.

To adapt this discussion to real fluid turbulence, one should examine the deep differences between our NLS-focusing inviscid unforced model (1) and the equations of inviscid fluid mechanics. As already said, in the case of the NLS-focusing model, if the amplitude of the fluctuations is above a certain value over a sufficiently large coherent domain, the instability sets in and leads to self-similar blow-up. In the case of the incompressible Euler equations for fluids, we suggest that the role of this instability is played by the Rayleigh instability of shear flows [53]. As is well known, this Rayleigh instability requires that, in a parallel flow, the velocity field presents an inflection point in its dependence with respect to the normal coordinate to the velocity. If this happens, an instability can develop. Because the Euler equations are formulated without any intrinsic scales of space and of velocity, the existence of an instability relies only on the local properties of the flow and not on external parameters or other quantities. Therefore, the onset of instability in a turbulent flow can depend only on dimensionless combinations built with local parameters of the velocity field. In fluids, the instability follows a Rayleigh-like criterion that involves second derivatives of the main

velocity field with respect to a coordinate (or coordinates) locally perpendicular to this field. For a random velocity field, this yields in principle a two-dimensional manifold that defines the local instability. Because the criterion is defined on surfaces, the growth of local singularities in turbulent fluids occurs with finite probability and depends on the local geometry of the velocity fluctuations in the flow. This implies that incoming singularities fill a finite proportion of the probability distribution functions of fluid acceleration signals, as is observed in turbulent flows [5]. This also agrees with the long observed, but as far as we know unexplained, sensitivity of real turbulent flows to detailed macroscopic features, such as changes in boundary conditions in the von Karman flow [54], for instance, something we interpret as also changing the geometry of those large-scale features and finally the probability of the occurrence of singularities.

IV. DISCUSSION

We have presented a model equation with many remarkable properties, making it a promising template for investigating the role of intermittencies in real fluid turbulence. The fluctuations of the solutions of Eq. (1) display indeed strong analogies with real fluid turbulence. In particular, they exhibit a well-defined Kolmogorov spectrum in an "inertial range" between the injection at large scales and dissipation at small scales. Moreover, the model shows a phenomenon of strong intermittency that results from the random occurrence of quasisingularities that are stopped before the final blow-up by a viscouslike term present in the model. This shows well that the occurrence of singularities for the "inviscid" part of the equation of motion is a way to explain how both dissipation and intermittency occur in such a turbulent system. The flux of a conserved quantity from large to small scales can somehow be linked to the random occurrence of coherent structures, the quasisingularities, with a well-defined time dependence, which is hard—if not impossible—to find by looking only at space- and time-averaged quantities. Preliminary numerical studies in two and three space dimensions support the present scenario positively. More specifically, for two space dimensions and a nonlinearity $n = 2$, one observes the phenomenology of Figs. 4 and 6 qualitatively. Nevertheless, for three space dimensions and $n = 1$, a slight difference occurs: in some situations, the intermittent behavior of the mean dissipation rate is missing because at almost every time the probability of observing an event is close to 1; thus a continuous curve replaces the intermittent behavior of Fig. 5(b). These results will be presented in detail elsewhere. We emphasize that in the current inviscid model, the space dimensions may be arbitrarily chosen as long as $D > 2/n$, while the fluid case is usually restricted to the pertinent three-dimensional situation.

Finally, to make a more specific connection between our model and real fluid turbulence, we notice that if intermittency is linked to finite-time singularities in both cases, the relevant fluctuations must exhibit a tight relationship between large amplitudes and short time. This kind of relationship does appear in the short-range behavior of the structure functions: such functions show the same change of qualitative behavior at a small radius both for NLS and recorded data in large wind tunnels, a subject that we plan to discuss in a separate publication.

ACKNOWLEDGMENT

Y.P. and S.R. acknowledge FONDECYT Grant No. 1181382, and S.R. acknowledges the Gaspard Monge Visiting Professor Program of École Polytechnique (France).

[1] G. K. Batchelor and A. A. Townsend, The nature of turbulent motion at large wave-numbers, Proc. R. Soc. London, Ser. A **199**, 238 (1949).

[2] C. Meneveau and K. R. Sreenivasan, The multifractal spectrum of the dissipation field in turbulent flows, Nucl. Phys. B, Proc. Suppl. **2**, 49 (1987).

[3] D. Buaria, A. Pumir, E. Bodenschatz, and P. K. Yeung, Extreme velocity gradients in turbulent flows, New J. Phys. **21**, 043004 (2019)
[4] U. Frisch, *Turbulence: The Legacy of A. N. Kolmogorov* (Cambridge University Press, Cambridge, 1996).
[5] Y. Pomeau, M. Le Berre, and T. Lehner, A case of strong nonlinearity: Intermittency in highly turbulent flows, C. R. Mécan. **347**, 342 (2019).
[6] L. Lichtenstein, Über einige existenzprobleme der hydrodynamik. Mat. Z. Phys. **23**, 89 (1925).
[7] N. Gunther, On the motion of fluid in a moving container, Izv. Akad. Nauk USSR, Ser. Fiz. Mat. **20**, 1323 (1927).
[8] J. Leray, Essai sur le mouvement d'un fluide visqueux emplissant l'espace, Acta Math. **63**, 193 (1934).
[9] Originally, Leray suggested the existence of finite-time singularities for an incompressible viscous fluid, which does not occur in either the Navier-Stokes equation or the Euler equation. Interestingly, Leray may have first introduced finite-time singularities of the type of Eq. (4) (see Sec. 20 of Ref. [8]).
[10] L. Onsager, Statistical hydrodynamics, Il Nuovo Cimento **6**, 279 (1949).
[11] G. L. Eyink and K. R. Sreenivasan, Onsager and the theory of hydrodynamic turbulence, Rev. Mod. Phys. **78**, 87 (2006).
[12] P. Debue, V. Shukla, D. Kuzzay, D. Faranda, E.-W. Saw, F. Daviaud, and B. Dubrulle, Dissipation, intermittency, and singularities in incompressible turbulent flows, Phys. Rev. E **97**, 053101 (2018).
[13] B. Dubrulle, Beyond Kolmogorov cascades, J. Fluid Mech. **867**, 1 (2019).
[14] E. D. Siggia, Collapse and amplification of a vortex filament, Phys. Fluids **28**, 794 (1985).
[15] A. Pumir and E. D. Siggia, Vortex dynamics and the existence of solutions to the Navier-Stokes equations, Phys. Fluids **30**, 1606 (1987).
[16] H. K. Moffatt and Y. Kimura, Towards a finite-time singularity of the Navier-Stokes equations. part 1. Derivation and analysis of dynamical system, J. Fluid Mech. **861**, 930 (2019).
[17] H. K. Moffatt and Y. Kimura, Towards a finite-time singularity of the Navier-Stokes equations. part 2. Vortex reconnection and singularity evasion, J. Fluid Mech. **870**, R1 (2019).
[18] H. K. Moffatt, Singularities in fluid mechanics, Phys. Rev. Fluids **4**, 110502 (2019).
[19] J. Eggers, The role of singularities in hydrodynamics, Phys. Rev. Fluids **3**, 110503 (2018).
[20] M. Brachet, M. Meneguzzi, A. Vincent, H. Politano, and P. L. Sulem, Numerical evidence of smooth self-similar dynamics for three dimensional ideal flows, Phys. Fluids A **4**, 2845 (1992).
[21] J. D. Gibbon, The three-dimensional Euler equations: Where do we stand? Physica D **237**, 1894 (2008).
[22] A. C. Newell and V. E. Zakharov, Rough Sea Foam, Phys. Rev. Lett. **69**, 1149 (1992).
[23] Y. Pomeau and M. Le Berre, Nonlinearity and nonequilibrium together in Nature: wind waves in the open ocean, Eur. Phys. J. D **62**, 73 (2011).
[24] G. Düring, C. Josserand, G. Krstulovic, and S. Rica, Strong turbulence for vibrating plates: Emergence of a Kolmogorov spectrum, Phys. Rev. Fluids **4**, 064804 (2019).
[25] S. Dyachenko, A. C. Newell, A. Pushkarev, and V. E. Zakharov, Optical turbulence: weak turbulence, condensates and collapsing filaments in the nonlinear Schrödinger equation, Physica D **57**, 96 (1992).
[26] M. V. Goldman, Rev. Mod. Phys. **56**, 709 (1984).
[27] D. Russel, D. F. DuBois, and H. A. Rose, Collapsing-Caviton Turbulence in One Dimension, Phys. Rev. Lett. **56**, 1758 (1986).
[28] A. C. Newell, D. A. Rand, and D. Russell, Turbulent dissipation rates and the random occurrence of coherent events, Phys. Lett. A **132**, 112 (1988).
[29] A. C. Newell, D. A. Rand, and D. Russell, Turbulent transport and the random occurrence of coherent events, Physica D **33**, 281 (1988).
[30] B. Rumpf and A. C. Newell, Intermittency as a consequence of turbulent transport in nonlinear systems, Phys. Rev. E **69**, 026306 (2004).
[31] B. Rumpf, A. C. Newell, and V. E. Zakharov, Turbulent Transfer of Energy by Radiating Pulses, Phys. Rev. Lett. **103**, 074502 (2009).
[32] Y. Pomeau and M. Le Berre, Blowing-up solutions of the axisymmetric Euler equations for an incompressible fluid, arXiv:1901.09426.
[33] Y. Pomeau, Singularité dans l'évolution du fluide parfait', C. R. Acad. Sci. Paris **321**, 407 (1995).
[34] J. Bec and K. Khanin, Burgers turbulence, Phys. Rep. **447**, 1 (2007).

[35] P. Manneville, Statistical properties of chaotic solutions of a one-dimensional model for phase turbulence, Phys. Lett. A **84**, 129 (1981).
[36] Y. Pomeau, A. Pumir, and P. Pelce, Intrinsic stochasticity with many degrees of freedom, J. Stat. Phys. **37**, 39 (1984).
[37] P. Coullet, L. Gil, and J. Lega, Defect-Mediated Turbulence, Phys. Rev. Lett. **62**, 1619 (1989).
[38] M. Bartuccelli, P. Constantin, C. R. Doering, J. D. Gibbon, and M. Gisselfalt, Hard turbulence in a finite dimensional dynamical system? Phys. Lett. A **142**, 349 (1989).
[39] M. Bartuccelli, P. Constantin, C. R. Doering, J. D. Gibbon, and M. Gisselfalt, On the possibility of soft and hard turbulence in the complex Ginzburg-Landau equation, Physica D **44**, 421 (1990).
[40] B. J. LeMesurier, G. C. Papanicolaou, C. Sulem, and P. L. Sulem, Focusing and multi-focusing solutions of the nonlinear Schrödinger equation, Physica D **31**, 78 (1988).
[41] C. J. Budd, S. Chen, and R. D. Russell, New self-similar solutions of the nonlinear Schrödinger equation with moving mesh methods, J. Comput. Phys. **152**, 756 (1999).
[42] C. Sulem and P.-L. Sulem, *The Nonlinear Schrödinger Equation* (Springer-Verlag, New York, 1999).
[43] V. I. Talanov, Self-focusing of wave beams in nonlinear media, JETP Lett. **2**, 138 (1965).
[44] V. E. Zakharov, Collapse of Langmuir waves, Zh. Eksp. Teor. Fiz. **62**, 1745 (1972) [Sov. Phys. JETP **35**, 908 (1972)].
[45] In 1D, this average reads $S_k(t) \equiv \frac{1}{2}(|\hat{\psi}_k|^2 + |\hat{\psi}_{-k}|^2)$.
[46] K. R. Sreenivasan, On the scaling of the turbulence energy dissipation rate, Phys. Fluids **27**, 1048 (1984).
[47] S. Nazarenko, *Wave Turbulence*, Lecture Notes in Physics Vol. 825 (Springer, Berlin, 2011).
[48] T. S. Lundgren, Strained spiral vortex model for turbulent structures, Phys. Fluids **25**, 2193 (1982).
[49] Y. Cuypers, A. Maurel, and P. Petitjeans, Vortex Burst as a Source of Turbulence, Phys. Rev. Lett. **91**, 194502 (2003).
[50] E. Falcon, S. G. Roux, and C. Laroche, On the origin of intermittency in wave turbulence, Europhys. Lett. **90**, 34005 (2010).
[51] S. Chibbaro and C. Josserand, Elastic wave turbulence and intermittency, Phys. Rev. E **94**, 011101(R) (2016).
[52] A. N. Kolmogorov, Dissipation of energy in the locally isotropic turbulence, Dokl. Akad. Nauk SSSR **30**, 301 (1941) [Proc. R. Soc. London **434**, 9 (1991) (in particular, see the second footnote on page 10)].
[53] P. G. Drazin and W. H. Reid, *Hydrodynamic Stability* (Cambridge University Press, Cambridge, 2010).
[54] O. Cadot, Y. Couder, A. Daerr, S. Douady, and A. Tsinober, Energy injection in closed turbulent flows: Stirring through boundary layers versus inertial stirring, Phys. Rev. E **56**, 427 (1997).